$$u=\alpha_1\left(\frac{B}{z}\right)^{1/3}, \tag{1}$$

$$b(z)=\alpha_2 z, \quad l=\alpha_3 z, \tag{2}$$

where $\alpha_1, \alpha_2, \ldots$ are constants and the specific buoyancy flux B is assumed to be the sole governing parameter representing the source. Since verifications of Eqs. (1) and (2) have been reported on numerous occasions,[19] pertinent measurements were not attempted in the present study. However, plume descent rates were measured for different plume diameters d_0 and the results were used to delineate conditions under which the point-plume approximation is valid.

On the premise of (1) and (2), turbulent quantities within a plume generated by a source of finite diameter d_0 can be written as

$$u=\left(\frac{B}{z}\right)^{1/3} f_1\left(\frac{d_0}{z}\right), \tag{3}$$

$$b=z f_2\left(\frac{d_0}{z}\right), \quad l=z f_3\left(\frac{d_0}{z}\right), \tag{4}$$

where $f_1, f_2, \ldots$ are functions, with f_1, f_2, and f_3 assuming constant values α_1, α_2, and α_3 as $d_0 \to 0$. In addition, for a point plume, the location h of the first plume front below the source and the maximum plume width b_m at a time t after the initiation can be written as

$$h=\alpha_4 (Bt^3)^{1/4}, \tag{5}$$

$$b_m=\alpha_5 (Bt^3)^{1/4}, \tag{6}$$

using the corresponding expressions for a finite-diameter plume which can also be written in the spirit of (3) and (4). For example, the position of the first plume front becomes

$$h=(Bt^3)^{1/4} f_4\left[\frac{d_0}{(Bt^3)^{1/4}}\right], \tag{7}$$

which, in the point-plume limit $d_0/(Bt^3)^{1/4} \to 0$ (i.e., at small d_0 or large t) yields $f_3 \to \alpha_4$. On the other hand, in the asymptotic limit $d_0/(Bt^3)^{1/4} \to \infty$, it is possible to expect $f_4 \to (Bt^3)^{1/4}/d_0$ corresponding to the case of convection from horizontally homogeneous sources (Fernando *et al.*[35]). Thus, the descent of the plume from a finite-diameter source is expected to follow asymptotic forms of $t^{3/2}$ at small times and $t^{3/4}$ at large times. The transition between two regimes can be used to obtain an idea of the onset of plume diameter effects for the flow evolution. Figure 9 shows a plot of $h/(Bt^3)^{1/4}$ vs $d_0/(Bt^3)^{1/4}$, for several experiments carried out with different source diameters. Note that, in an average sense, the point plume scaling (5) is approached when $d_0/(Bt^3)^{1/4} < 0.14$, whence $h/(Bt^3)^{1/4} = \alpha_4 \approx 1.7$. Thus, the evolution of a finite-sized plume becomes asymptotically similar to that of a point plume when $h > 12 d_0$. At lesser depths, the finite diameter effects can be important. Also, it is noted that experimental results at large $d_0/(Bt^3)^{1/4}$ limit do not converge to the horizontally homogeneous case, possibly because of the continued dominance of entrainment flow in the $d_0/(Bt^3)^{1/4}$ range investigated.

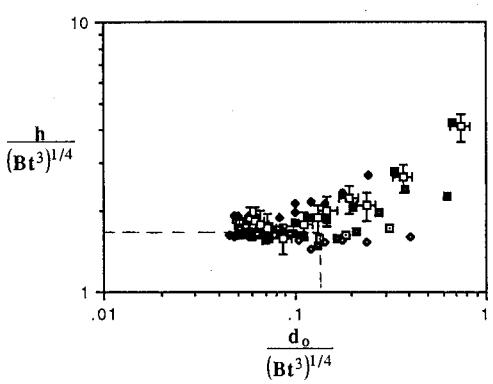

FIG. 9. A plot of the normalized position of the first plume front vs normalized source diameter drawn to check the validity of (7). The horizontal line represents the point plume case. The experimental parameters are □ and ◇ —$d_0 = 0.6$ cm; ⊡ and ◆ —$d_0 = 1.27$ cm; ■ and □—$d_0 = 2.54$ cm.

C. Descent of a point plume in the presence of rotation

As described in Sec. II, the maximum plume width b_m and the depth h of the plume front were measured using the video records taken during the experiments performed in the square tank and by analyzing them frame by frame. Concentration contours of the plume fluid were constructed using the laser-induced fluorescence technique and the contour line representing 5% of the maximum concentration (evaluated at each horizontal imaging level) was used to evaluate the plume envelope and hence h and b_m. The results were arranged concurrent with (5) and (6), in the nondimensional form,

$$\frac{h}{\left(\frac{B}{\Omega^3}\right)^{1/4}}=\alpha_4(\Omega t)^{3/4}, \tag{8}$$

and

$$\frac{b_m}{\left(\frac{B}{\Omega^3}\right)^{1/4}}=\alpha_5(\Omega t)^{3/4}. \tag{9}$$

The experimental results are shown in Figs. 10 and 11.

In Fig. 10, the solid line drawn through the data (in log–log form) indicates the 3/4 slope predicted by (8). Close

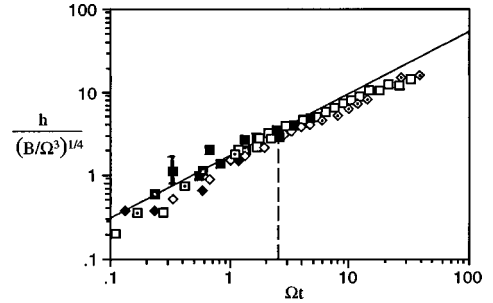

FIG. 10. A plot of the nondimensional plume descent vs nondimensional time. The estimated time at which deviation from the $t^{3/4}$ law occurs is indicated. ⊡ $\rho_p = 1.058$ g cm^{-3}, $\Omega = 0.5$ rad s^{-1}; ◆ $\rho_p = 1.058$, $\Omega = 0.7$; □ $\rho_p = 1.058$, $\Omega = 0.33$; ◇ $\rho_p = 1.014$, $\Omega = 0.4$; ■ $\rho_p = 1.016$, $\Omega = 0.5$; □ $\rho_p = 1.016$, $\Omega = 0.7$.